

Nanostructure-assisted optical tweezers toward microspectroscopic polymer analysis

メタデータ	言語: English 出版者: Springer Nature 公開日: 2021-04-06 キーワード (Ja): キーワード (En): optical tweezers, thermoresponsive polymer chains, polystyrene nanospheres, Raman, fluorescence microspectroscopy, localized surface plasmon, black silicon 作成者: 東海林, 竜也, 坪井, 泰之 メールアドレス: 所属: Osaka City University, Kanagawa University, Osaka City University
URL	https://ocu-omu.repo.nii.ac.jp/records/2020451

Nanostructure-assisted optical tweezers for microspectroscopic polymer analysis

Tatsuya Shoji, Yasuyuki Tsuboi

Citation	Polymer Journal. 53(2); 271-281.
Issue Date	2021-02
Published	2020-09-17
Type	Journal Article
Textversion	author
Rights	<p>This is the accepted manuscript version of an article published in Polymer Journal. The final published version is available online at: https://doi.org/10.1038/s41428-020-00410-w.</p> <p>See Springer Nature terms for use of archived author accepted manuscripts of subscription articles. https://www.nature.com/nature-research/editorial-policies/self-archiving-and-licensing-to-publish</p>
DOI	10.1038/s41428-020-00410-w

Self-Archiving by Author(s)

Placed on: Osaka City University Repository

Nanostructure-assisted optical tweezers toward microspectroscopic polymer analysis

Tatsuya SHOJI^{1),2)}*, Yasuyuki TSUBOI¹⁾

1) *Division of Molecular Materials Science, Graduate School of Science, Osaka City University, 3-3-138 Sugimoto, Sumiyoshi, Osaka 558-8585, Japan*

2) *Department of Chemistry, Faculty of Science, Kanagawa University, 2946 Tsuchiya, Hiratsuka 259-1293, Japan*

* Corresponding Author: t-shoji@kanagawa-u.ac.jp

Running Head

Optical trapping of polymer chains

Abstract

Raman/fluorescence microspectroscopies on individual polymer chains and nanobeads dissolved in solution will become a powerful analytical method to study molecular structure and characteristics of them. Toward this motivation, we focused on Raman microspectroscopy for optically trapped soft matter. A tightly focused near-infrared laser beam formed a microassembly of thermoresponsive polymer chains such as poly(*N*-isopropylacrylamide) due to a local photothermal effect and optical force. By using this method, we developed a determination technique of the polymer concentration in the polymer microassembly. Furthermore, we demonstrated a molecular condensation and detection technique based on the microassembly on the plasmonic nanostructures. For this molecular condensation and detection, localized surface plasmon play an essential role in the enhancement of optical force and a local temperature elevation around the plasmonic nanostructures. Finally, toward novel manipulation methods of smaller soft nanomaterials, nanostructured semiconductor-assisted (NASSCA) optical tweezers will be introduced. In this paper, we reviewed the optical manipulation methods of polymer chains and nanobeads and their applications toward analytical chemistry.

Key Words

optical tweezers, thermoresponsive polymer chains, polystyrene nanospheres, Raman/fluorescence microspectroscopy, localized surface plasmon, black silicon

Introduction

Thermoresponsive polymer chains which have both hydrophilic and hydrophobic groups in their side chains exhibit demixing and remixing in solution. The most intensively studied thermoresponsive polymer is poly(*N*-isopropylacrylamide) (PNIPAM).¹ An aqueous PNIPAM solution follows the lower critical solution temperature (LCST) phase separation behaviors and exhibit demixing from a homogeneous to an inhomogeneous condition upon heating and remixing upon cooling. The phase separation has been widely studied by using static/dynamic light scattering,²⁻⁸ small angle neutron scattering (SANS),^{9,10} FT-IR/Raman spectroscopies,¹¹⁻¹³ dielectric relaxation,^{14,15} NMR,^{16,17} calorimetry,^{18,19} and so on. We have investigated the dynamics of phase separation by using laser T-jump method with transient photometry and single molecular fluorescence microscopy.²⁰⁻²⁵ According to such previous studies, PNIPAM are homogeneously dissolved as hydrated coil structures below LCST. When heated above LCST, PNIPAM undergoes a phase separation from coil to dehydrated globular structures. Subsequently, the polymer chains undergo aggregation because of a hydrophobic interaction, forming the phase separation into polymer-rich and water-rich microdroplets. For such characteristic behavior, structural information on PNIPAM chains in polymer-rich microdroplets is essential for the medical applications such as tissue engineering and drug delivery systems.²⁶⁻³⁰

Raman spectroscopic studies on the polymer-rich microdroplet has been reported by Maeda et al. in 2003.³¹ The droplet was formed by heating a dense aqueous PNIPAM solution (10–60 wt% corresponding to 6–80 mmol/L). Since the droplet with several tens of micrometers in size was physically adsorbed on glass surface, Raman signals from the droplet was obtainable with highly accurate positioning. However, polymer chains in the dense droplet are entangled with each other, being no longer dilute solution. In order to provide new insight into the phase

separation behavior, another way to access the polymer-rich microdroplets in the dilute solution is in high demand. However, since the size of droplets was only a few micrometers, these are continuously fluctuated in solution. In such situation, it is difficult to obtain signals from the individual microdroplets.

Thus, we focus on the optical tweezers combined with Raman microspectroscopy. Optical tweezers, which use a tightly focused laser beam, can grab micrometer-sized objects such as living cells, viruses, and polymer microspheres and the Nobel prize in Physics 2018 was awarded to an investigator, Arthur Ashkin.³²⁻³⁷ By using this technique, we have investigated Raman microspectroscopic analysis on an optically trapped thermoresponsive polymer-rich microdroplet,^{38,39} providing new way to determine the polymer concentration of the microdroplet.⁴⁰ Furthermore, molecular condensation and detection methods using the hydrophobic polymer-rich microdroplets were proposed in the previous report.⁴¹ In this review, we described optical trappings of soft matters and their analytical applications. The principle of optical force exerted on nanomaterials will be briefly introduced. Polymer chains dissolved in solution were optically trapped, leading to a microassembly at the focal point. By combining Raman microspectroscopy, we can access the structural information on individual polymer-rich microdroplets. Furthermore, to achieve an efficient optical trapping of soft nanomaterials, we introduced recent hot topics of optical manipulation which uses plasmonic nanostructures; plasmonic optical tweezers. Finally, we described our novel non-plasmonic optical manipulation using nanostructured black silicon; nanostructured semiconductor-assisted (NASSCA) optical tweezers.^{42,43}

Methods

According to Newton's third law, light refracted on a small particle exerts optical force F on the particle due to a change in the momentum of light. In the Rayleigh scattering regime (particle radius $r \ll$ light wavelength λ), optical force F on the nanoparticle can be approximately obtained by the sum of three forces; a gradient force F_{grad} , an absorption force F_{abs} , and a scattering force F_{scat} (Fig. 1(a)). The absorption and scattering forces are repulsive forces that carry the particle along the light propagation:^{44,45}

$$F_{\text{scat}} = \hat{\mathbf{k}} \frac{4\pi^3 n_m}{c \varepsilon_0^2 \lambda^4} |\alpha|^2 I \quad (1)$$

$$F_{\text{abs}} = \hat{\mathbf{k}} \frac{2\pi}{c \varepsilon_0 \lambda} \text{Im}[\alpha] I \quad (2)$$

Where ε_0 is the dielectric constant in vacuum, α is the complex polarizability of the particle obtained from Clausius-Mossotti relation, n_m is the refractive index of the surrounding medium, I is the intensity of laser light, c is the speed of light, and $\hat{\mathbf{k}}$ is the unit vector in the direction of propagation of the light. The gradient force F_{grad} is an attractive force that pulls the nanoparticle in the focal point of laser light:

$$F_{\text{grad}} = \frac{1}{c n_m \varepsilon_0} \text{Re}[\alpha] \nabla I \quad (3)$$

In the Rayleigh regime, gradient force overcomes both scattering and absorption forces because of small polarizability of a nanoparticle, leading to the optical trapping of nanoparticles. However, for the stable trapping, the potential energy U of the gradient force overcomes the thermal energy $k_B T$ (k_B is the Boltzmann constant and T is the absolute temperature; at room temperature, $k_B T \sim 4.1 \times 10^{-21}$ J), because a nanoparticle is continuously fluctuated by Brownian motion (Fig. 1(b)). Equation 3 describes three important points for the stable trapping of a nanoparticle: (i) according to polarizability, the refractive index of the medium is smaller than that of trapping target, (ii) the grip (trapping strength) of optical tweezers becomes stronger with increasing laser light intensity I , (iii) stable optical trapping becomes harder with decreasing the

particle radius r ($|U| \propto r^3$). For instance, Hosokawa et al. reported optical potential U for 100 nm sized polystyrene nanospheres with a tightly focused laser beam.⁴⁶ They experimentally determined the potential to be $105 k_B T$ when a near-infrared laser beam ($\lambda = 1064$ nm, $P = 300$ mW) was tightly focused in water with a high-numerical aperture objective lens (N.A. = 1.25).

Fig. 2 shows the optical setup for microspectroscopic studies on optically trapped polymer chains. A continuous wave (cw) laser beam ($\lambda = 1064$ nm) was used for optical trapping, being tightly focused into the sample solution through a high numerical aperture objective lens of an inverted optical microscope. To obtain spectroscopic signals from the trapped nanoparticles, a cw visible laser beam was coaxially introduced into the microscope. The signals were detected with a charge-coupled device (CCD) camera equipped with a polychromator. The details have been already described in elsewhere. By using such optical setup, we demonstrated optical trapping of soft nanomaterials such as proteins,⁴⁷⁻⁴⁹ amino acids,⁵⁰ poly(lactic-*co*-glycolic acid) PLGA,^{51,52} and so on.

Results & Discussion

Optical trapping of polymer chains

Optical tweezers were mainly used for non-contact and non-destructive manipulation of micrometer-sized objects such as living cells, polystyrene microsphere, and so on. In 1990s, several research groups have reported optical tweezers for polymer chains dissolved in solution. Table 1 shows representative trapping targets reported in literatures.⁵³⁻⁵⁹ In general, since polymer chains in solution held in a partially extended state, their polarizability is quite small in comparison with that of a rigid microsphere. Consequently, a tightly focused laser beam with high laser intensity is required for trapping them. For instance, Rubinsztein-Dunlop et al. found molecular weight dependence of optical trapping by using a poly(ethylene oxide) (PEO) aqueous solution.⁵⁵ They determined a minimum laser power required for the stable optical trapping of

PEO to be 0.29 W ($M_v = 900,000$) and 0.53 W ($M_v = 300,000$), respectively. However, PEO with $M_v = 100,000$ was never trapped even though they used intense laser beam (0.70 W). These results were good agreement with theoretical calculation of optical force exerted on PEO.

Masuhara et al. first demonstrated optical trapping of PNIPAM in which pyrene was labeled as a fluorescence molecular probe.^{56,57} Pyrene-labeled PNIPAM in an aqueous solution exhibits excimer emission at high concentration both inter- and intra-polymer aggregation of polymer chains. A tightly focused laser irradiation trapped the polymer chains, leading to the microassembly formation at the focal point of laser beam. Fluorescence microspectroscopy of the microassembly indicated the increment of excimer emission as laser irradiation time. They discussed the formation mechanism caused by photothermal effect by water and optical force. The detail of the trapping mechanism will be described later.

Optical tweezers for PNIPAM combined with confocal Raman microspectroscopy

We investigated structural analysis of optically trapped PNIPAM with confocal Raman microspectroscopy.⁴⁰ Fig. 3(a) shows bright field microscopic observation during optical trapping of PNIPAM (2.5 mmol/L, M_w 150,000) by using a 1064 nm laser beam (0.19 W). With the start of near-infrared laser irradiation, a micrometer-sized particle was formed at the focal point. With irradiation time, the size of particle became gradually larger up to 10 μm in diameter. Turning off laser irradiation, the particle was immediately dissolved in solution. The particle size increased with laser power. However, below 0.12 W, we have never observed any trapping signals.

We successfully obtained the Raman spectrum of the single particle. Fig. 3(b) shows the Raman spectrum in the high wavenumber region (2800 – 3800 cm^{-1}) corresponding to the CH stretching modes of the PNIPAM main chain (2800 – 3050 cm^{-1}) and those of the OH stretching modes (3100 – 3800 cm^{-1}). With increasing the near-infrared laser power, the Raman scattering

intensity of CH stretching modes increased because of the increment of PNIPAM concentration in the microparticle. Fig. 3(c) shows the expanded Raman spectra in the 2850 – 3050 cm^{-1} regions. The intensity ratio between Raman bands at 2925 and 2944 cm^{-1} , which were ascribed to the asymmetric CH stretching modes, sensitively reflected the hydration/dehydration of polymer main chain. The inversed intensity ratio from the optically formed PNIPAM microparticle means that PNIPAM in the microparticle took a dehydrated globule state. This result was further supported by the Raman microspectroscopic studies below 1600 cm^{-1} on the PNIPAM microparticle previously described in elsewhere.³⁸

Here, we discussed the trapping mechanism of PNIPAM. A near-infrared laser beam at 1064 nm was tightly focused into a PNIPAM aqueous solution, exerting optical force on the polymer chain and leading to the local temperature elevation by light absorption of H_2O . Since water has an absorption band at 1200 nm corresponding to an overtone of the OH stretching mode, temperature rises around the focal point by a photothermal effect. The quantitative evaluation of the temperature elevation is still under debate. For instance, Ito et al. applied fluorescence correlation microspectroscopy for the quantitative analysis.⁶⁰ They determined the temperature elevation to be 23 ± 1 K by 1064 nm laser irradiation at 1 W. Such local temperature elevation is enough to induce phase separation around the focal point. The optical force exerted on the dehydrated polymer chains, leading to the optical trapping of them at the focal point. The trapped polymer chains aggregates with each other due to hydrophobic interaction, resulting in the formation of a single PNIPAM-rich microdroplet at the focal point.

Determination method of polymer concentration in PNIPAM polymer-rich microdroplet with optical tweezers

By using optical tweezers combined with Raman microspectroscopy, we can determine the polymer concentration of a single polymer-rich microdroplet.⁴⁰ We obtained Raman scattering

intensity ratio between the CH stretching modes of the PNIPAM main chain ($2800 - 3050 \text{ cm}^{-1}$) and those of the OH stretching modes ($3100 - 3800 \text{ cm}^{-1}$) from the droplet. Using standard lines, we determined the polymer concentration in a droplet. Fig. 3(d) shows the near-infrared laser intensity dependence of the polymer concentration of the microdroplet. Below 0.12 W , a microdroplet was never formed because weak optical force and low temperature elevation. For instance, a polymer concentration of the microdroplet formed in a 3.6 wt\% PNIPAM aqueous solution was determined to be ca. 37 wt\% at 0.12 W of laser power, suggesting that a microdroplet held abundant water molecules even above LCST. As increasing laser power, the concentration became higher up to $60\text{-}70 \text{ wt\%}$. This result would be caused by an optical force and a photothermal effect. To shed further light on the mechanism, optical trapping of PNIPAM in heavy water (D_2O) would provide grateful information. Since heavy water is transparent at 1064 nm ,⁶⁰ we discussed it only by an effect of optical force.³⁸ In D_2O , Raman microspectroscopy suggested that a PNIPAM microparticle formed by optical force took a dehydration structure.

As described above, optical tweezers combined with Raman microspectroscopy will be powerful analytical method for the thermoresponsive polymer chains dissolved in solution. However, the optical force dramatically decreases with decrease of trapping target sizes. In order to demonstrate optical trapping of smaller nanoparticle, localized surface plasmon has attracted much attention.

Plasmonic optical tweezers

According to the equation (3), EM field of incident light should become higher to amplify an optical force. Recently, localized surface plasmon (LSP) provides a new way for the efficient optical trapping of nanoparticles.⁶¹⁻⁶⁶ LSP of noble metallic nanostructures leads to an enhancement effect of resonant light, resulting in the increase of the optical force exerted on the nanomaterials around the plasmonic nanostructures. Following early demonstrations, plasmonic

optical trapping (POT) has undergone rapid growth. We have demonstrated plasmonic optical tweezers for nanoparticles such as quantum dots,⁶⁷ polystyrene nanospheres,^{68,69} J-/H-aggregates,⁷⁰ DNA,^{71,72} and polymer chains.⁷³ Furthermore, we applied POT of PNIPAM for molecular condensation and microspectroscopic detection as described in the next section.⁴¹ POT has three advantages in comparison with the conventional optical tweezers (Fig. 4): (1) laser light intensity required for the stable optical trapping becomes lower because of enhancement effect of localized surface plasmon, (2) the diffusive motion of a trapped nanoparticle is tightly restricted in the plasmonic nanospace, which is smaller than the diffraction limit of light, and (3) POT has potential for the combination of other plasmonic applications such as highly sensitive spectroscopies,^{74–78} biosensors,^{79,80} and photochemical reactions.^{81–85} In this review, we focused on the POT of PNIPAM chains and analytical applications of it for molecular condensation and detections.

Plasmonic optical trapping of PNIPAM

As a plasmon nanostructure, we used a gold nanopyramidal dimer array on a glass substrate.^{86–90} This plasmonic nanostructure is fabricated by an angular-resolved nanosphere lithography method. A resonance extinction band appeared in the near-infrared region (700 ~ 1000 nm). Accordingly, the electric field of incident near-infrared light was enhanced up to 10^4 times between the nano-gaps ($|E|^2/|E_0|^2 \sim 10^4$); gap-mode LSP. The optical system is almost the same as in Fig. 2, but the laser light at $\lambda = 808$ nm instead of 1064 nm was used for LSP excitation.

Fig. 5(a) shows bright-field observations during POT of PNIPAM.⁷³ A plasmon excitation light was loosely focused on the gold nanopyramidal dimer array, leading to the a PNIPAM microassembly formation only inside the excitation area. Stopping the excitation, the microassembly dissolved in solution. In order to study the trapping behavior, we carried out fluorescence microspectroscopic analysis on POT of PNIPAM labeled with a fluorescence

molecular probe (Fig. 5(b)), whose fluorescence was sensitive to the surrounding polar environment. The maximum wavelength of the fluorescence changes a blue shift by decreasing polarity of a surrounding medium because of an intramolecular charge transfer. As expected, the fluorescence wavelength exhibits a blue shift by phase separation. The fluorescence intensity during POT of PNIPAM (red line in Fig. 5(c)) became higher than that without POT (black line), meaning that local concentration on the plasmonic nanostructures increased because of the formation of PNIPAM microassembly. Furthermore, we found that the fluorescence spectrum slightly showed a blue shift (Fig. 5(c)), suggesting that plasmon excitation results in the enhancement of optical force and phase separation. This behavior is caused by a photothermal effect upon plasmon excitation. We carefully estimated the temperature elevation during plasmon excitation by means of fluorescence correlation microspectroscopy to be 8.0 ± 1.0 K at 1.0 kW/cm² of plasmon excitation. Furthermore, we evaluated the spatial gradient of temperature around plasmon excitation area to be 0.5 K/ μ m. This temperature elevation with huge temperature gradient should induce thermal convection and thermophoresis.

Based on these effects (optical force, thermophoresis, and thermal convection), we proposed the formation mechanism of PNIPAM microassembly. Local temperature elevation around the excited plasmonic nanostructures induces phase separation of PNIPAM, leading to the formation of polymer-rich microdroplets. Such microdroplets are optically trapped, since optical force becomes stronger as the trapping target size gets larger. Thermal convection supports POT by supplying the polymers from outside to inside of the plasmon excitation area. Thus, POT of PNIPAM forms a hydrophobic microassembly on a plasmonic nanostructures. For the detail of the formation mechanism, we will focus on a spatial temperature profile during POT in future studies.

Molecular condensation and detection by using PNIPAM microassembly

We applied POT of PNIPAM for the condensation of organic molecules sparsely dissolved in aqueous solution (Fig. 6(a)). Fig. 6(b) shows fluorescence spectrum of rhodamine B (RhB) condensed in a PNIPAM microassembly formed on plasmonic nanostructures.⁴¹ Fluorescence intensity with plasmon excitation became 140 times higher than that without plasmon excitation because of molecular condensation. Considering the distribution coefficient K_{poly} of polycyclic aromatic hydrocarbons between PNIPAM and aqueous solution ($K_{\text{poly}} = [\text{solute}]_{\text{poly}}/[\text{solute}]_{\text{solution}} = 10^2\sim 10^3$), the fluorescence enhancement mainly results in the increase of RhB concentration in the microassembly. Fig. 6(c) shows a temporal profile of the fluorescence intensity monitored at 576 nm in the molecular condensation process. Since the rapid microassembly formation within 1 second, the fluorescence detection also responds quickly. We succeeded in the RhB detection at the nano-molar level (1.0×10^{-9} mol/L). This method also condensed and detected other fluorescent molecules such as crystal violet and acid red 88. Furthermore, we demonstrated Raman measurements of chlorophenols condensed in the PNIPAM microassembly. Since such condensation is dependent on hydrophobic properties between analytes and polymer chains such as the polymer concentration, molecular weight, chemical structures of side chains. This work will become a powerful method to detect a variety of organic molecules.

Nanostructured semiconductor-assisted (NASSCA) optical tweezers

While POT has great advantages over the conventional optical tweezers, some problems should be for further development: (1) a severe fabrication process of fine-shape plasmonic nanostructures with high reproducibility and uniformity over large area, (2) a material cost because of the usage of gold and silver, and (3) temperature elevation. In particular, thermophoresis induced by photothermal effect is hardly negligible because it frequently prevents

stable POT. In 2017, we developed novel non-plasmonic optical manipulation method using nanostructured black silicon (B-Si);⁹¹⁻⁹⁶ nanostructured semiconductor-assisted (NASSCA) optical tweezers.⁴² Crozier et al. have recently reported the optical trappings of polymer nanospheres using silicon nano-antenna.⁹⁷ These methods have great potential for the non-plasmonic optical manipulation method of nanomaterials. In the last part of this review, we briefly introduced NASSCA optical tweezers. There are nanoneedles on the surface of B-Si which can amplify the incident light by a factor of ca. 5 due to multiple light scattering. Although the enhancement effect ($|E|^2/|E_0|^2$) of B-Si is much smaller than that of plasmonic nanostructures (10^4), the trapping efficiency (stiffness) of NASSCA optical tweezers overcomes that of POT due to reduction of photothermal effect.

Fig. 7(a-d) shows representative fluorescence micrographs during NASSCA optical trapping of polystyrene nanospheres (diameter 500 nm) on a B-Si surface (Fig. 7(e)).⁴² We used commercially available fluorescent dye-doped polystyrene nanospheres (Invitrogen™, F8813). Since the dye molecules in the nanospheres have an absorption band around 505 nm and an emission band around 515 nm, we can obtain fluorescence micrographs with a mercury lamp. The Turning on laser light irradiation ($\lambda = 808$ nm, 320 kW/cm²), polystyrene nanospheres were trapped one by one, leading to the assembly formation of the nanospheres with irradiation time. When the turning off the irradiation, the nanospheres were released and dissipated in solution. Furthermore, we found the regular packing of numerous polystyrene nanospheres with lower laser powers ($10\sim 20$ kW/cm²) (Fig. 7(f)).⁷² We believe that NASSCA optical tweezers with the intriguing behaviors promises an interesting new avenue exploiting the manipulation of nanomaterials beyond POT.

Conclusion

We conclude this review with description of the perspectives of nanostructure-assisted optical tweezers. Conventional optical tweezers combined with Raman microspectroscopy will provide new analytical method for a polymer-rich microdroplet of thermoresponsive polymer chains, which is continuously fluctuated in a dilute polymer solution above LCST. However, optical force of the conventional optical tweezers is frequently not enough to trap soft matter. To overcome this limitation, plasmonic optical tweezers has been growing continuously since the early 2000s. During plasmon excitation, nanoparticles were efficiently trapped on the plasmonic nanostructures. For POT applications, soft matter such as proteins, DNA, and polymer chains, will be attracted because plasmonics has widely used in the field of chemistry and biosensors. We found that POT of PNIPAM led to the formation of a phase-separated microdroplet on the plasmonic nanostructures. The hydrophobic microdroplet can act as a platform to condense and detect the sparsely distributed organic molecules in solution. This novel analytical method will become a versatile tool by combining conventional plasmonic ultra-highly sensitive spectroscopies such as surface enhanced Raman spectroscopy (SERS). However, a photothermal effect by plasmon excitation frequently hinders the stable optical trapping of soft nanomaterials because of thermophoresis and thermal convection. A hot topic on optical manipulation is the non-plasmonic silicon nanostructure-assisted optical manipulation. We developed NASSCA optical tweezers for capturing polystyrene nanospheres, led to the 2D photonic like microassembly formation of the nanospheres. We offer an outlook on the future directions of such nanostructure-assisted optical tweezers to be the protein crystallization, the nanoparticle sorting, photonic crystal fabrication, and so on. We believe that plasmonic optical tweezers and NASSCA optical tweezers will become a useful manipulation tool for nanoparticles and smaller macromolecules as conventional optical tweezers have been proven to be a valuable micromanipulation tool.

Acknowledgement

The authors acknowledge the contributions from our collaborators. This work was partly supported by JSPS KAKENHI Grant Numbers JP17K04974, JP18K14254, and JP16H06507 in Scientific Research on Innovative Areas “Nano-Material Manipulation and Structural Order Control with Optical Forces” and “Molecular Engine” (JP19H05402). Authors are grateful for financial supports from the SEI (Sumitomo Electric Industry) group Foundation and the CANON Foundation.

References

1. Heskins, M. & Guillet, J. E. Solution Properties of Poly(N-isopropylacrylamide). *J. Macromol. Sci. Part A - Chem.* **2**, 1441–1455 (1968).
2. Fujishige, S., Kubota, K. & Ando, I. Phase transition of aqueous solutions of poly (N-isopropylacrylamide) and poly (N-isopropylmethacrylamide). *J. Phys. Chem.* **93**, 3311–3313 (1989).
3. Wu, C. & Zhou, S. Thermodynamically Stable Globule State of a Single Poly(N-isopropylacrylamide) Chain in Water. *Macromolecules* **28**, 5388–5390 (1995).
4. Wang, X., Qiu, X. & Wu, C. Comparison of the Coil-to-Globule and the Globule-to-Coil Transitions of a Single Poly(N-isopropylacrylamide) Homopolymer Chain in Water. *Macromolecules* **31**, 2972–2976 (1998).
5. Wu, C. & Wang, X. Globule-to-Coil Transition of a Single Homopolymer Chain in Solution. *Phys. Rev. Lett.* **80**, 4092–4094 (1998).
6. Cheng, H., Shen, L. & Wu, C. LLS and FTIR studies on the hysteresis in association and dissociation of poly(N-isopropylacrylamide) chains in water. *Macromolecules* **39**, 2325–2329 (2006).
7. Kujawa, P., Segui, F., Shaban, S., Diab, C., Okada, Y., Tanaka, F. & Winnik, F. M. Impact of end-group association and main-chain hydration on the thermosensitive properties of hydrophobically modified telechelic poly(N-isopropylacrylamides) in water. *Macromolecules* **39**, 341–348 (2006).
8. Kuang, C., Yusa, S. & Sato, T. Micellization and Phase Separation in Aqueous Solutions of Thermosensitive Block Copolymer Poly(N-isopropylacrylamide)- b -poly(N-vinyl-2-pyrrolidone) upon Heating. *Macromolecules* **52**, 4812–4819 (2019).
9. Meier-Koll, A., Pipich, V., Busch, P., Papadakis, C. M. & Müller-Buschbaum, P. Phase separation in semidilute aqueous poly(N-isopropylacrylamide) solutions. *Langmuir* **28**, 8791–8798 (2012).
10. Stieger, M., Pedersen, J. S., Lindner, P. & Richtering, W. Are thermoresponsive

- microgels model systems for concentrated colloidal suspensions? A rheology and small-angle neutron scattering study. *Langmuir* **20**, 7283–7292 (2004).
11. Maeda, Y., Higuchi, T. & Ikeda, I. Change in Hydration State during the Coil–Globule Transition of Aqueous Solutions of Poly(N -isopropylacrylamide) as Evidenced by FTIR Spectroscopy. *Langmuir* **16**, 7503–7509 (2000).
 12. Plamper, F. a, Steinschulte, A. a, Hofmann, C. H., Drude, N., Mergel, O., Herbert, C., Erberich, M., Schulte, B., Winter, R. & Richtering, W. Toward Copolymers with Ideal Thermosensitivity: Solution Properties of Linear, Well-De fi ned Polymers of N-Isopropyl Acrylamide and N,N- Diethyl Acrylamide. *Macromolecules* **45**, 8021–8026 (2012).
 13. Ahmed, Z., Gooding, E. A., Pimenov, K. V, Wang, L. & Asher, S. A. UV resonance Raman determination of molecular mechanism of poly(N-isopropylacrylamide) volume phase transition. *J. Phys. Chem. B* **113**, 4248–4256 (2009).
 14. Ono, Y. & Shikata, T. Hydration and Dynamic Behavior of Poly(N -isopropylacrylamide)s in Aqueous Solution: A Sharp Phase Transition at the Lower Critical Solution Temperature. *J. Am. Chem. Soc.* **128**, 10030–10031 (2006).
 15. Füllbrandt, M., Ermilova, E., Asadujjaman, A., Hölzel, R., Bier, F. F., von Klitzing, R. & Schönhals, A. Dynamics of Linear Poly(N -isopropylacrylamide) in Water around the Phase Transition Investigated by Dielectric Relaxation Spectroscopy. *J. Phys. Chem. B* **118**, 3750–3759 (2014).
 16. Starovoytova, L. & Spěvácěk, J. Effect of time on the hydration and temperature-induced phase separation in aqueous polymer solutions. ¹H NMR study. *Polymer (Guildf)*. **47**, 7329–7334 (2006).
 17. Spěvácěk, J., Konefał, R. & Čadová, E. NMR Study of Thermoresponsive Block Copolymer in Aqueous Solution. *Macromol. Chem. Phys.* **217**, 1370–1375 (2016).
 18. Tiktopulo, E. I.; Bychkova, V. E.; Ricka, J.; Ptitsyn, O. B. Cooperativity of the Coil-Globule Transition in a Homopolymer: Microcalorimetric Study of Poly(N-isopropylacrylamide). *Macromolecules* **27**, 2879–2882 (1994).
 19. Zhou, X., Li, J., Wu, C. & Zheng, B. Constructing the phase diagram of an aqueous solution of poly(n-isopropyl acrylamide) by controlled microevaporation in a nanoliter microchamber. *Macromol. Rapid Commun.* **29**, 1363–1367 (2008).
 20. Tsuboi, Y., Yoshida, Y., Okada, K. & Kitamura, N. Phase separation dynamics of aqueous solutions of thermoresponsive polymers studied by a laser T-jump technique. *J. Phys. Chem. B* **112**, 2562–2565 (2008).
 21. Tsuboi, Y., Tada, T., Shoji, T. & Kitamura, N. Phase-Separation Dynamics of Aqueous Poly (N -isopropylacrylamide) Solutions: Characteristic Behavior of the Molecular

- Weight and Concentration Dependences. *Macromol. Chem. Phys.* **213**, 1879–1884 (2012).
22. Tada, T., Katsumoto, Y., Goossens, K., Uji-i, H., Hofkens, J., Shoji, T., Kitamura, N. & Tsuboi, Y. Accelerating the Phase Separation in Aqueous Poly(N -isopropylacrylamide) Solutions by Slight Modification of the Polymer Stereoregularity: A Single Molecule Fluorescence Study. *J. Phys. Chem. C* **117**, 10818–10824 (2013).
 23. Tada, T., Hirano, T., Ute, K., Katsumoto, Y., Asoh, T.-A., Shoji, T., Kitamura, N. & Tsuboi, Y. Effects of Syndiotacticity on the Dynamic and Static Phase Separation Properties of Poly(N -isopropylacrylamide) in Aqueous Solution. *J. Phys. Chem. B* **120**, 7724–7730 (2016).
 24. Matsumoto, M., Wakabayashi, R., Tada, T., Asoh, T.-A., Shoji, T., Kitamura, N. & Tsuboi, Y. Rapid Phase Separation in Aqueous Solution of Temperature-Sensitive Poly(N , N -diethylacrylamide). *Macromol. Chem. Phys.* **217**, 2576–2583 (2016).
 25. Matsumoto, M., Tada, T., Asoh, T.-A., Shoji, T., Nishiyama, T., Horibe, H., Katsumoto, Y. & Tsuboi, Y. Dynamics of the Phase Separation in a Thermoresponsive Polymer: Accelerated Phase Separation of Stereocontrolled Poly(N , N -diethylacrylamide) in Water. *Langmuir* **34**, 13690–13696 (2018).
 26. Schmaljohann, D. Thermo- and pH-responsive polymers in drug delivery. *Adv. Drug Deliv. Rev.* **58**, 1655–70 (2006).
 27. Nagase, K., Yamato, M., Kanazawa, H. & Okano, T. Poly(N-isopropylacrylamide)-based thermoresponsive surfaces provide new types of biomedical applications. *Biomaterials* **153**, 27–48 (2018).
 28. Van Vlierberghe, S., Dubruel, P. & Schacht, E. Biopolymer-based hydrogels as scaffolds for tissue engineering applications: A review. *Biomacromolecules* **12**, 1387–1408 (2011).
 29. Doberenz, F., Zeng, K., Willems, C., Zhang, K. & Groth, T. Thermoresponsive polymers and their biomedical application in tissue engineering-A review. *J. Mater. Chem. B* **8**, 607–628 (2020).
 30. Xu, X., Liu, Y., Fu, W., Yao, M., Ding, Z., Xuan, J., Li, D., Wang, S., Xia, Y. & Cao, M. Poly(N-isopropylacrylamide)-Based Thermoresponsive Composite Hydrogels for Biomedical Applications. *Polymers (Basel)*. **12**, 580 (2020).
 31. Maeda, Y., Yamamoto, H. & Ikeda, I. Phase Separation of Aqueous Solutions of Poly(N -isopropylacrylamide) Investigated by Confocal Raman Microscopy. *Macromolecules* **36**, 5055–5057 (2003).
 32. Ashkin, A. & Dziedzic, J. M. Optical Levitation by Radiation Pressure. *Appl. Phys. Lett.* **19**, 283–285 (1971).

33. Ashkin, A., Dziedzic, J. M., Bjorkholm, J. E. & Chu, S. Observation of a single-beam gradient force optical trap for dielectric particles. *Opt. Lett.* **11**, 288 (1986).
34. Ashkin, A., Dziedzic, J. M. & Yamane, T. Optical trapping and manipulation of single cells using infrared laser beams. *Nature* **330**, 769–771 (1987).
35. Ashkin, A. Optical trapping and manipulation of neutral particles using lasers. *Proc. Natl. Acad. Sci.* **94**, 4853–4860 (1997).
36. Ashkin, A., Dziedzic, J. M., Bjorkholm, J. E. & Chu, S. Observation of a single-beam gradient force optical trap for dielectric particles. *Opt. Lett.* **11**, 288 (1986).
37. Ashkin, A. & Dziedzic, J. Optical trapping and manipulation of viruses and bacteria. *Science (80-.)*. **235**, 1517–1520 (1987).
38. Tsuboi, Y., Nishino, M., Sasaki, T. & Kitamura, N. Poly(N-Isopropylacrylamide) Microparticles Produced by Radiation Pressure of a Focused Laser Beam: A Structural Analysis by Confocal Raman Microspectroscopy Combined with a Laser-Trapping Technique. *J. Phys. Chem. B* **109**, 7033–7039 (2005).
39. Tsuboi, Y., Nishino, M., Matsuo, Y., Ijiro, K. & Kitamura, N. Phase separation of aqueous poly(vinyl methyl ether) solutions induced by the photon pressure of a focused near-infrared laser beam. *Bull. Chem. Soc. Jpn.* **80**, 1926–1931 (2007).
40. Shoji, T., Nohara, R., Kitamura, N. & Tsuboi, Y. A method for an approximate determination of a polymer-rich-domain concentration in phase-separated poly(N-isopropylacrylamide) aqueous solution by means of confocal Raman microspectroscopy combined with optical tweezers. *Anal. Chim. Acta* **854**, 118–121 (2015).
41. Shoji, T., Sugo, D., Nagasawa, F., Murakoshi, K., Kitamura, N. & Tsuboi, Y. Highly Sensitive Detection of Organic Molecules on the Basis of a Poly(N - isopropylacrylamide) Microassembly Formed by Plasmonic Optical Trapping. *Anal. Chem.* **89**, 532–537 (2017).
42. Shoji, T., Mototsuji, A., Balčytis, A., Linklater, D., Juodkazis, S. & Tsuboi, Y. Optical tweezing and binding at high irradiation powers on black-Si. *Sci. Rep.* **7**, 12298 (2017).
43. Hanasaki, I., Shoji, T. & Tsuboi, Y. Regular Assembly of Polymer Nanoparticles by Optical Trapping Enhanced with a Random Array of Si Needles for Reconfigurable Photonic Crystals in Liquid. *ACS Appl. Nano Mater.* **2**, 7637–7643 (2019).
44. Svoboda, K. & Block, S. M. Optical trapping of metallic Rayleigh particles. *Opt. Lett.* **19**, 930 (1994).
45. Kendrick, M. J., McIntyre, D. H. & Ostroverkhova, O. Wavelength dependence of optical tweezer trapping forces on dye-doped polystyrene microspheres. *J. Opt. Soc. Am. B* **26**, 2189–2198 (2009).
46. Hosokawa, C., Yoshikawa, H. & Masuhara, H. Optical assembling dynamics of

- individual polymer nanospheres investigated by single-particle fluorescence detection. *Phys. Rev. E* **70**, 061410 (2004).
47. Tsuboi, Y., Shoji, T. & Kitamura, N. Crystallization of Lysozyme Based on Molecular Assembling by Photon Pressure. *Jpn. J. Appl. Phys.* **46**, L1234–L1236 (2007).
 48. Tsuboi, Y., Shoji, T., Nishino, M., Masuda, S., Ishimori, K. & Kitamura, N. Optical manipulation of proteins in aqueous solution. *Appl. Surf. Sci.* **255**, 9906–9908 (2009).
 49. Shoji, T., Kitamura, N. & Tsuboi, Y. Resonant Excitation Effect on Optical Trapping of Myoglobin: The Important Role of a Heme Cofactor. *J. Phys. Chem. C* **117**, 10691–10697 (2013).
 50. Tsuboi, Y., Shoji, T. & Kitamura, N. Optical Trapping of Amino Acids in Aqueous Solutions. *J. Phys. Chem. C* **114**, 5589–5593 (2010).
 51. Yan, H., Hou, Y.-F., Niu, P.-F., Zhang, K., Shoji, T., Tsuboi, Y., Yao, F.-Y., Zhao, L.-M. & Chang, J.-B. Biodegradable PLGA nanoparticles loaded with hydrophobic drugs: confocal Raman microspectroscopic characterization. *J. Mater. Chem. B* **3**, 3677–3680 (2015).
 52. Yang, J., Zhang, R.-N., Liu, D.-J., Zhou, X., Shoji, T., Tsuboi, Y. & Yan, H. Laser trapping/confocal Raman spectroscopic characterization of PLGA-PEG nanoparticles. *Soft Matter* **14**, 8090–8094 (2018).
 53. Borowicz, P., Hotta, J., Sasaki, K. & Masuhara, H. Laser-controlled association of poly(N-vinylcarbazole) in organic solvents: Radiation pressure effect of a focused near-infrared laser beam. *J. Phys. Chem. B* **101**, 5900–5904 (1997).
 54. Borowicz, P., Hotta, J., Sasaki, K. & Masuhara, H. Chemical and Optical Mechanism of Microparticle Formation of Poly(N -vinylcarbazole) in N , N -Dimethylformamide by Photon Pressure of a Focused Near-Infrared Laser Beam. *J. Phys. Chem. B* **102**, 1896–1901 (1998).
 55. Singer, W., Nieminen, T. A., Heckenberg, N. R. & Rubinsztein-Dunlop, H. Collecting single molecules with conventional optical tweezers. *Phys. Rev. E* **75**, 011916 (2007).
 56. Ishikawa, M., Misawa, H., Kitamura, N. & Masuhara, H. Poly(N-isopropylacrylamide) Microparticle Formation in Water by Infrared Laser-Induced Photo-Thermal Phase Transition. *Chem. Lett.* **22**, 481–484 (1993).
 57. Ishikawa, M., Misawa, H., Kitamura, N., Fujisawa, R. & Masuhara, H. Infrared Laser-Induced Photo-Thermal Phase Transition of an Aqueous Poly(N -isopropylacrylamide) Solution in the Micrometer Dimension. *Bull. Chem. Soc. Jpn.* **69**, 59–66 (1996).
 58. Masuo, S., Yoshikawa, H., Nothofer, H.-G., Grimsdale, A. C., Scherf, U., Müllen, K. & Masuhara, H. Assembling and orientation of polyfluorenes in solution controlled by a focused near-infrared laser beam. *J. Phys. Chem. B* **109**, 6917–6921 (2005).

59. Nabetani, Y., Yoshikawa, H., Grimsdale, A. C., Müllen, K. & Masuhara, H. Effects of optical trapping and liquid surface deformation on the laser microdeposition of a polymer assembly in solution. *Langmuir* **23**, 6725–6729 (2007).
60. Ito, S., Sugiyama, T., Toitani, N., Katayama, G. & Miyasaka, H. Application of fluorescence correlation spectroscopy to the measurement of local temperature in solutions under optical trapping condition. *J. Phys. Chem. B* **111**, 2365–2371 (2007).
61. Volpe, G., Quidant, R., Badenes, G. & Petrov, D. Surface plasmon radiation forces. *Phys. Rev. Lett.* **96**, 238101 (2006).
62. Galloway, C. M., Kreuzer, M. P., Aćimović, S. S., Volpe, G., Correia, M., Petersen, S. B., Neves-Petersen, M. T. & Quidant, R. Plasmon-Assisted Delivery of Single Nano-Objects in an Optical Hot Spot. *Nano Lett.* **13**, 4299–4304 (2013).
63. Shoji, T. & Tsuboi, Y. Plasmonic Optical Tweezers toward Molecular Manipulation: Tailoring Plasmonic Nanostructure, Light Source, and Resonant Trapping. *J. Phys. Chem. Lett.* **5**, 2957–2967 (2014).
64. Shoji, T. & Tsuboi, Y. Plasmonic optical trapping of soft nanomaterials such as polymer chains and DNA: micro-patterning formation. *Opt. Rev.* **22**, 137–142 (2015).
65. Dienerowitz, M., Mazilu, M. & Dholakia, K. Optical manipulation of nanoparticles: A review. *J. Nanophotonics* **2**, 021875 (2008).
66. Wu, J. & Gan, X. Three dimensional nanoparticle trapping enhanced by surface plasmon resonance. *Opt. Exp.* **18**, 27619–27626 (2010).
67. Tsuboi, Y., Shoji, T., Kitamura, N., Takase, M., Murakoshi, K., Mizumoto, Y. & Ishihara, H. Optical Trapping of Quantum Dots Based on Gap-Mode-Excitation of Localized Surface Plasmon. *J. Phys. Chem. Lett.* **1**, 2327–2333 (2010).
68. Shoji, T., Shibata, M., Kitamura, N., Nagasawa, F., Takase, M., Murakoshi, K., Nobuhiro, A., Mizumoto, Y., Ishihara, H. & Tsuboi, Y. Reversible Photoinduced Formation and Manipulation of a Two-Dimensional Closely Packed Assembly of Polystyrene Nanospheres on a Metallic Nanostructure. *J. Phys. Chem. C* **117**, 2500–2506 (2013).
69. Shoji, T., Mizumoto, Y., Ishihara, H., Kitamura, N., Takase, M., Murakoshi, K. & Tsuboi, Y. Plasmon-Based Optical Trapping of Polymer Nano-Spheres as Explored by Confocal Fluorescence Microspectroscopy: A Possible Mechanism of a Resonant Excitation Effect. *Jpn. J. Appl. Phys.* **51**, 092001 (2012).
70. Mototsuji, A., Shoji, T., Wakisaka, Y., Murakoshi, K., Yao, H. & Tsuboi, Y. Plasmonic optical trapping of nanometer-sized J- /H- dye aggregates as explored by fluorescence microspectroscopy. *Opt. Exp.* **25**, 13617 (2017).
71. Shoji, T., Saitoh, J., Kitamura, N., Nagasawa, F., Murakoshi, K., Yamauchi, H., Ito, S.,

- Miyasaka, H., Ishihara, H. & Tsuboi, Y. Permanent Fixing or Reversible Trapping and Release of DNA Micropatterns on a Gold Nanostructure Using Continuous-Wave or Femtosecond-Pulsed Near-Infrared Laser Light. *J. Am. Chem. Soc.* **135**, 6643–6648 (2013).
72. Shoji, T., Itoh, K., Saitoh, J., Kitamura, N., Yoshii, T., Murakoshi, K., Yamada, Y., Yokoyama, T., Ishihara, H. & Tsuboi, Y. Plasmonic Manipulation of DNA using a Combination of Optical and Thermophoretic Forces: Separation of Different-Sized DNA from Mixture Solution. *Sci. Rep.* **10**, 3349 (2020).
73. Toshimitsu, M., Matsumura, Y., Shoji, T., Kitamura, N., Takase, M., Murakoshi, K., Yamauchi, H., Ito, S., Miyasaka, H., Nobuhiro, A., Mizumoto, Y., Ishihara, H. & Tsuboi, Y. Metallic-Nanostructure-Enhanced Optical Trapping of Flexible Polymer Chains in Aqueous Solution As Revealed by Confocal Fluorescence Microspectroscopy. *J. Phys. Chem. C* **116**, 14610–14618 (2012).
74. McNay, G., Eustace, D., Smith, W. E., Faulds, K. & Graham, D. Surface-Enhanced Raman Scattering (SERS) and Surface-Enhanced Resonance Raman Scattering (SERRS): A Review of Applications. *Appl. Spectrosc.* **65**, 825–837 (2011).
75. Vo-Dinh, T., Wang, H.-N. & Scaffidi, J. Plasmonic nanoprobe for SERS biosensing and bioimaging. *J. Biophotonics* **3**, 89–102 (2010).
76. Alvarez-Puebla, R. a & Liz-Marzán, L. M. Traps and cages for universal SERS detection. *Chem. Soc. Rev.* **41**, 43–51 (2012).
77. Yuan, Y., Lin, Y., Gu, B., Panwar, N., Tjin, S. C., Song, J., Qu, J. & Yong, K. T. Optical trapping-assisted SERS platform for chemical and biosensing applications: Design perspectives. *Coord. Chem. Rev.* **339**, 138–152 (2017).
78. Schlücker, S. Surface-Enhanced Raman Spectroscopy: Concepts and Chemical Applications. *Angew. Chemie Int. Ed.* **53**, 4756–4795 (2014).
79. Fan, X., White, I. M., Shopova, S. I., Zhu, H., Suter, J. D. & Sun, Y. Sensitive optical biosensors for unlabeled targets: a review. *Anal. Chim. Acta* **620**, 8–26 (2008).
80. Peng, H. I. & Miller, B. L. Recent advancements in optical DNA biosensors: exploiting the plasmonic effects of metal nanoparticles. *Analyst* **136**, 436–447 (2011).
81. Ueno, K. & Misawa, H. Surface plasmon-enhanced photochemical reactions. *J. Photochem. Photobiol. C* **15**, 31–52 (2013).
82. Ueno, K., Juodkazis, S., Shibuya, T., Yokota, Y., Mizeikis, V., Sasaki, K. & Misawa, H. Nanoparticle plasmon-assisted two-photon polymerization induced by incoherent excitation source. *J. Am. Chem. Soc.* **130**, 6928–6929 (2008).
83. Brus, L. Noble metal nanocrystals: Plasmon electron transfer photochemistry and single-molecule Raman spectroscopy. *Acc. Chem. Res.* **41**, 1742–1749 (2008).

84. Ueno, K. & Misawa, H. Photochemical reaction fields with strong coupling between a photon and a molecule. *J. Photochem. Photobiol., A* **221**, 130–137 (2011).
85. Baffou, G. & Quidant, R. Nanoplasmonics for chemistry. *Chem. Soc. Rev.* **43**, 3898–907 (2014).
86. Nagasawa, F., Takase, M. & Murakoshi, K. Raman Enhancement via Polariton States Produced by Strong Coupling between a Localized Surface Plasmon and Dye Excitons at Metal Nanogaps. *J. Phys. Chem. Lett.* **5**, 14–19 (2014).
87. Li, X., Minamimoto, H. & Murakoshi, K. Electrochemical surface-enhanced Raman scattering measurement on ligand capped PbS quantum dots at gap of Au nanodimer. *Spectrochim. Acta - Part A Mol. Biomol. Spectrosc.* **197**, 244–250 (2018).
88. Takase, M., Nabika, H., Hoshina, S., Nara, M., Komeda, K.-I., Shito, R., Yasuda, S. & Murakoshi, K. Local thermal elevation probing of metal nanostructures during laser illumination utilizing surface-enhanced Raman scattering from a single-walled carbon nanotube. *Phys. Chem. Chem. Phys.* **15**, 4270–4274 (2013).
89. Takase, M., Ajiki, H., Mizumoto, Y., Komeda, K., Nara, M., Nabika, H., Yasuda, S., Ishihara, H. & Murakoshi, K. Selection-rule breakdown in plasmon-induced electronic excitation of an isolated single-walled carbon nanotube. *Nat. Photonics* **7**, 550–554 (2013).
90. Sawai, Y., Takimoto, B., Nabika, H., Ajito, K. & Murakoshi, K. Observation of a small number of molecules at a metal nanogap arrayed on a solid surface using surface-enhanced Raman scattering. *J. Am. Chem. Soc.* **129**, 1658–1662 (2007).
91. Gailevičius, D., Ryu, M., Honda, R., Lundgaard, S., Suzuki, T., Maksimovic, J., Hu, J., Linklater, D. P., Ivanova, E. P., Katkus, T., Anand, V., Malinauskas, M., Nishijima, Y., Hock Ng, S., Staliūnas, K., Morikawa, J. & Juodkazis, S. Tilted black-Si: ~0.45 form-birefringence from sub-wavelength needles. *Opt. Express* **28**, 16012 (2020).
92. Nishijima, Y., Komatsu, R., Ota, S., Seniutinas, G., Balčytis, A. & Juodkazis, S. Anti-reflective surfaces: Cascading nano/microstructuring. *APL Photonics* **1**, 076104 (2016).
93. Linklater, D. P., Haydous, F., Xi, C., Pergolesi, D., Hu, J., Ivanova, E. P., Juodkazis, S., Lippert, T. & Juodkazytė, J. Black-Si as a Photoelectrode. *Nanomaterials* **10**, 873 (2020).
94. Liu, X., Coxon, P. R., Peters, M., Hoex, B., Cole, J. M. & Fray, D. J. Black silicon: Fabrication methods, properties and solar energy applications. *Energy Environ. Sci.* **7**, 3223–3263 (2014).
95. Savin, H., Repo, P., von Gastrow, G., Ortega, P., Calle, E., Garín, M. & Alcobilla, R. Black silicon solar cells with interdigitated back-contacts achieve 22.1% efficiency. *Nat. Nanotechnol.* **10**, 624–628 (2015).

96. Oh, J., Yuan, H.-C. & Branz, H. M. An 18.2%-efficient black-silicon solar cell achieved through control of carrier recombination in nanostructures. *Nat. Nanotechnol.* **7**, 743–748 (2012).
97. Xu, Z., Song, W. & Crozier, K. B. Optical Trapping of Nanoparticles Using All-Silicon Nanoantennas. *ACS Photonics* **5**, 4993–5001 (2018).

Display Items & Figure legends

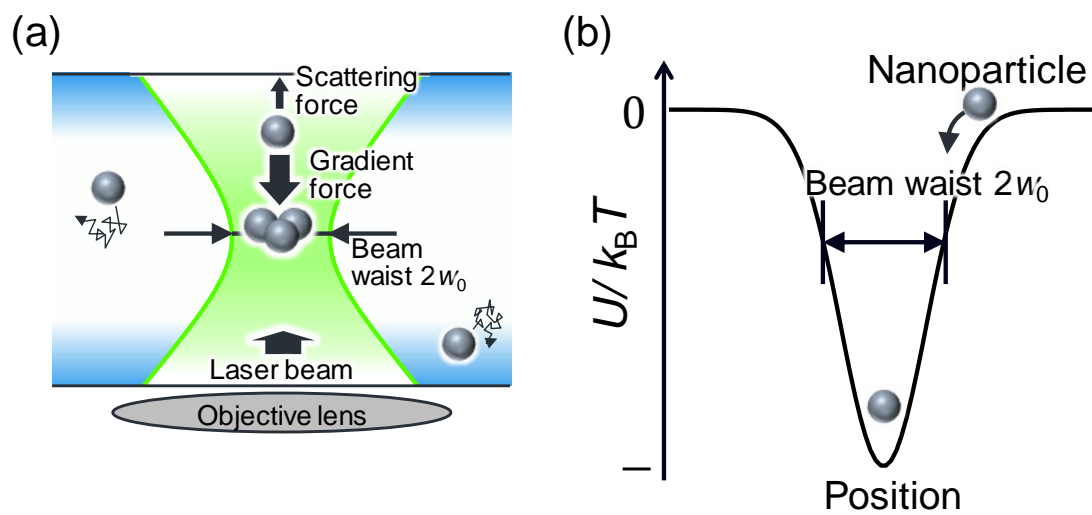


Fig. 1 Schematic illustrations of (a) optically trapped nanoparticles at the focal point of a tightly laser beam and (b) a potential curve of optical force.

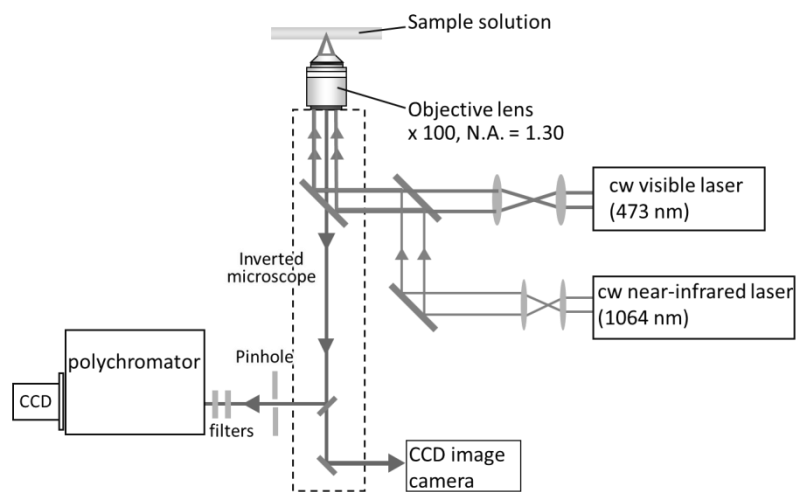


Fig 2. Experimental setup for optical tweezers with confocal Raman microspectroscopy.

Table 1. List of optically trapped polymer chains with optical tweezers.

Polymer chains	Ref.
poly(<i>N</i> -vinylcarbazole) and its derivatives	53, 54
poly(ethylene oxide)	55
poly(<i>N</i> -isopropylacrylamide) and its derivatives	38, 40, 56,57
poly(vinyl methyl ether)	39
polyfluorene	58,59

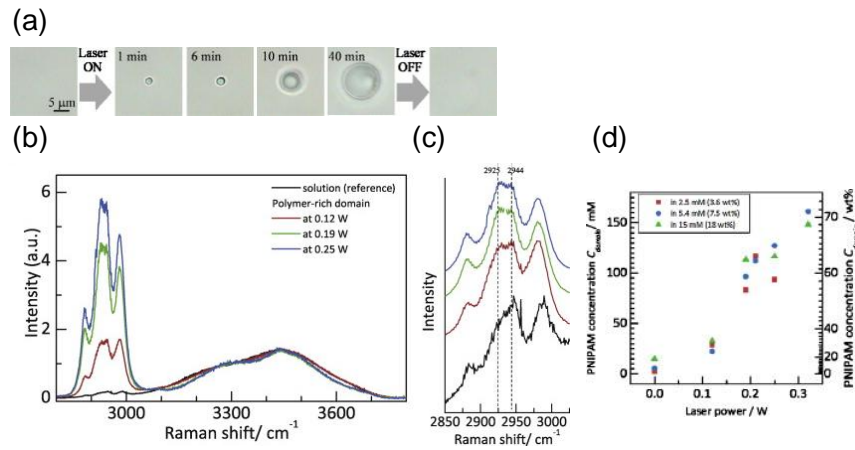


Fig 3. (a) Bright-field optical micrographs of a single phase-separated polymer-rich droplet formed by optical tweezers. (b) Raman spectra of the droplet at 0.12 W (red), 0.19 W (green), and 0.25 W (blue) of near-infrared laser power together with that of 2.5 mmol/L aqueous PNIPAM solution. (c) Expanded spectra of Fig. 3(b) for a 2850–3050 cm^{-1} region. PNIPAM concentration in a phase-separated polymer-rich droplet as a function of near-infrared laser power and solution concentration. Reprinted with permission from 40. Copyright 2015 Elsevier.

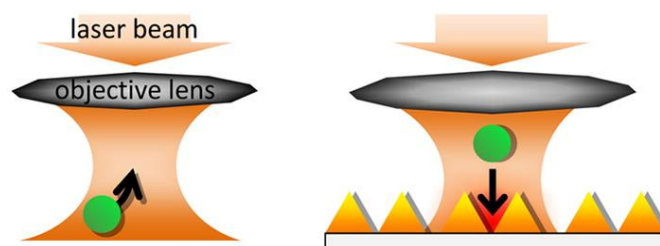


Fig. 4 Schematic illustrations of (left) conventional optical tweezers and (right) plasmonic optical tweezers. Reprinted with permission from ref 63. Copyright 2014 American Chemical Society.

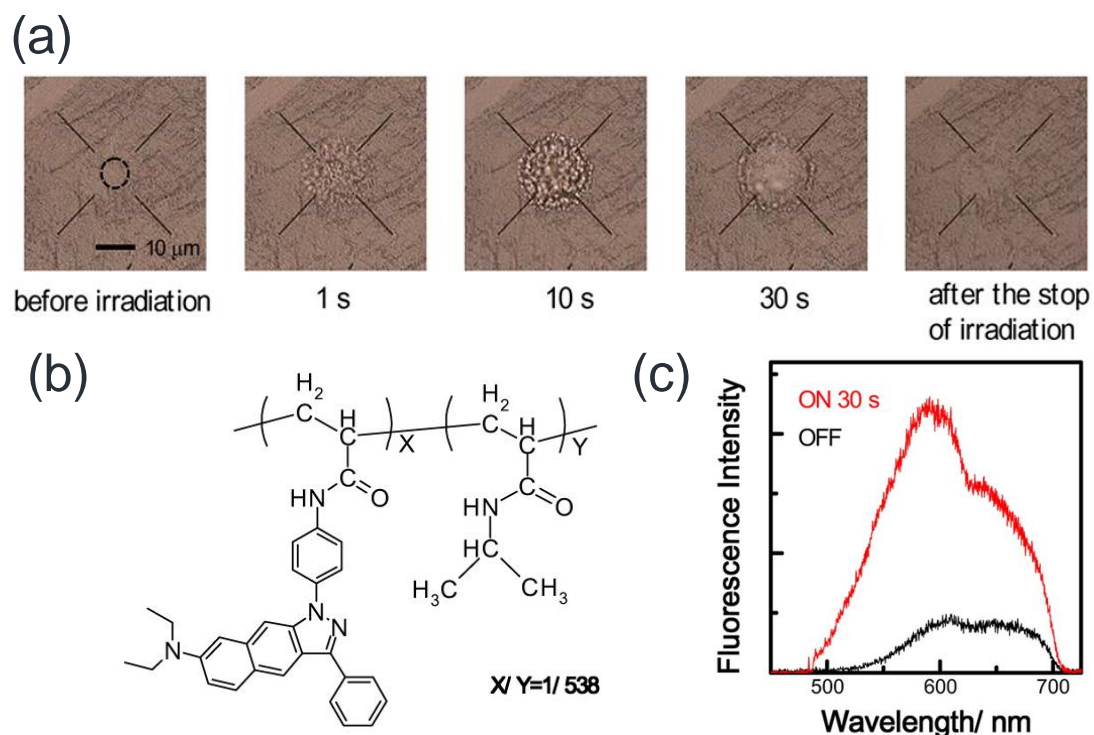


Fig. 5 (a) Bright-field optical micrographs during plasmonic optical trapping (POT) of PNIPAM. (b) Chemical structure of PNIPAM labeled with a fluorescence molecular probe. (c) Fluorescence spectra during POT (red) together with that without POT. Reprinted with permission from 73. Copyright 2012 American Chemical Society.

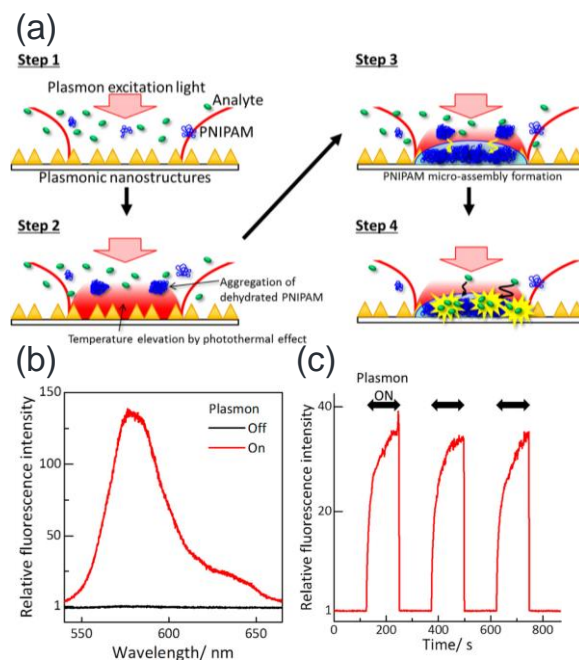


Fig. 6 (a) Schematic illustration of molecular condensation and detection by using PNIPAM microassembly formed by POT. (b) Fluorescence spectrum of Rhodamine B with (red) and without plasmon excitation (black). (c) Representative time profile of the fluorescence intensity. Reprinted with permission from 41. Copyright 2017 American Chemical Society.

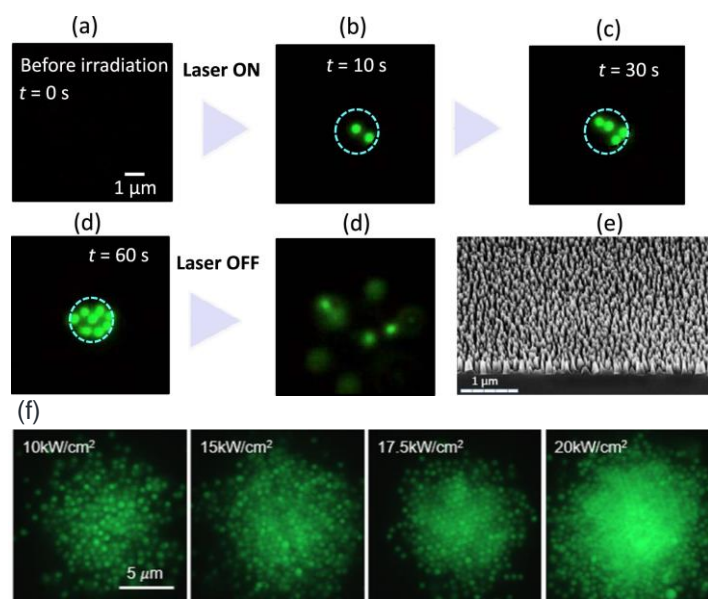


Fig. 7 (a-d) Fluorescence micrographs during NASSCA optical trapping of polystyrene nanospheres (500 nm in diameter) at 320 kW/cm^2 of laser intensity. (e) a SEM image of B-Si. Reprinted with permission from 42. Copyright 2017 Nature Springer. (f) Laser intensity dependence of NASSCA optical trapping of the nanospheres. Reprinted with permission from 43. Copyright 2019 American Chemical Society.